

that the charge conjugate $\psi_c = C\bar{\psi}^T$ of ψ does *not* belong to the same representation¹⁴ as ψ removes at once the crossing symmetry difficulties pointed out by Riazuddin *et al.*¹⁵ It is perhaps worth emphasizing that if the coupling suggested in Eq. (18) is replaced by the much simpler (and equally invariant) form

$$g\bar{\psi}\Phi\psi, \quad (32)$$

then the resulting theory gives exactly the same *results* as those of Salam *et al.*⁵ and Sakita *et al.*,⁶ except that there is now no conflict with the Bargmann-Wigner⁹ equations or crossing.¹⁶ The differing *predictions* of those theories and the present one for the baryon-meson vertex

¹⁴ That ψ_c transforms with the opposite sign to ψ for infinitesimal transformations of the type $i\gamma_\mu\gamma_5$ was noted by H. J. Lipkin and S. Meshkov, *Phys. Rev. Letters* **14**, 670 (1965), who independently discovered the spin transformations of Ref. 10 as a subgroup of $\tilde{U}(12)$, and suggested the name W spin.

¹⁵ Riazuddin, L. K. Pandit, and S. Okubo, University of Rochester Report U.R.-875-79 1965 (unpublished).

¹⁶ No difficulties with unitarity arise in this case, as there is no direct restriction on four-pion functions. In fact unitarity offers possible information on the four-point functions through the restrictions imposed by the symmetry on three-point functions.

lie entirely in the introduction of the momentum-dependent $P\tilde{U}(4)$ transformations which define the coupling in Eq. (18).

In view of the success of the present scheme it is most desirable to investigate its possible extension to other processes. The first and most crucial point to be made is that in general there is no immediate extension of the spin transformations to four point (or higher) functions¹⁷; this is essentially a theory of three-point functions. Any restrictions which the theory imposes on four-point functions must be through the implicit effects of restrictions on the three-point functions (e.g., through unitarity, or the decomposition of the amplitude into pole contributions with only three-point vertices). The three-meson interaction however should be amenable to treatment along the present lines, although the author has not yet succeeded in the endeavor to define this interaction in a way fully consistent with the above work.

¹⁷ The exceptions to this statement arise perhaps when particles of degenerate mass have collinear momenta, i.e., forward and backward scattering.

Σ Radiative Decay and the Angular Momentum of Σ Pionic Decay

M. BAZIN, H. BLUMENFELD, U. NAUENBERG, AND L. SEIDLITZ
*Princeton University, Princeton, New Jersey**

AND

R. J. PLANO AND S. MARATECK
Rutgers, The State University, New Brunswick, New Jersey†

AND

P. SCHMIDT
*Columbia University, New York, New York**

(Received 20 July 1965)

We have studied the pion spectrum in the $\Sigma^\pm \rightarrow n + \pi^\pm + \gamma$ decay in order to determine the angular-momentum channel of the Σ pionic decay. We discuss the results from measurements of a sample of 14 800 $\Sigma^+ \rightarrow \pi^+ + n$ decays and 25 000 $\Sigma^- \rightarrow \pi^- + n$ decays. After subtraction of the background, we find 26 Σ^+ radiative decays and 28 Σ^- radiative decays with $P_{c.m.} < 166$ MeV/c. The combination $\Sigma^+ \rightarrow \pi^+ + n$ decays via P wave and $\Sigma^- \rightarrow \pi^- + n$ decays via S wave is 45 times more likely than the combination $\Sigma^+ \rightarrow \pi^+ + n$ decays via S wave and $\Sigma^- \rightarrow \pi^- + n$ decays via P wave. This means that our result is 2.7 standard deviations in favor of the first combination.

RECENTLY some interest has been centered on a determination of the pion spectrum in the decay $\Sigma^\pm \rightarrow n + \pi^\pm + \gamma$. This comes about because the pion momentum spectrum in this decay is sensitive to the angular-momentum channel of the decay $\Sigma^\pm \rightarrow n + \pi^\pm$.¹ It is well

known that the $\Delta I = \frac{1}{2}$ rule for nonleptonic decays² combined with the experimental measurements on the α parameter and rates of the Σ decays³ predict that the $\Sigma^+ \rightarrow \pi^+ + n$ and the $\Sigma^- \rightarrow \pi^- + n$ decays must occur, respectively, through the S - and P -wave channels or

* Work supported by the U. S. Atomic Energy Commission.

† Work supported by the National Science Foundation.

¹ S. Barshay, U. Nauenberg, and J. Schultz, *Phys. Rev. Letters* **12**, 76 (1964). M. C. Li and G. A. Snow, Univ. of Maryland Technical Report No. 351 (unpublished). S. Barshay and R. E. Behrends, *Phys. Rev.* **114**, 931 (1959).

² M. Gell-Mann and A. Rosenfeld, *Ann. Rev. Nucl. Sci.* **7**, 407 (1959).

³ Bruce Cork, L. T. Kerth, W. A. Wenzel, J. W. Cronin, and R. L. Cool, *Phys. Rev.* **120**, 1000 (1960); R. D. Tripp, M. B. Watson, and M. Ferro-Luzzi, *Phys. Rev. Letters* **9**, 66 (1962).

vice versa. In addition, there are various predictions based on SU_3 or SU_6 which state that either the $\Sigma^+ \rightarrow \pi^+ + n$ S -wave decay amplitude is zero or the P -wave decay amplitude is zero.⁴ Hence a study of the pion momentum spectrum in the decays $\Sigma^\pm \rightarrow n + \pi^\pm + \gamma$, as presented here, can determine the validity of these predictions and bring an end to the ambiguity present in the triangle representation of the Σ decays.

The basic technique of the experiment has been described before.⁵ Essentially, it consists of the following steps:

1. Low-momentum Σ^- 's and Σ^+ 's were produced in $K^- - p$ interactions at rest in the 30-in. Columbia-BNL hydrogen bubble chamber.
2. All Σ decays were scanned and measured with film digitizing machines independently of how they looked on the scanning table as long as the projected length of the decay pion was more than 10 cm in any one of the three views and the Σ was clearly visible. In addition, in the case of Σ^+ decays, it was required that the decay track, if it stopped in the chamber, decay in the characteristic $\pi^+ \rightarrow \mu^+ \rightarrow e^+$ sequence. If not, the event was rejected as a decay of the type $\Sigma^+ \rightarrow p + \pi^0$.
3. All the measured events were sent through the NP54⁶ spatial reconstruction program. Events with measured decay track lengths < 10 cm or dips $\geq 60^\circ$ were rejected from further analysis. In addition we rejected all Σ^- events where the Σ^- length was ≥ 0.95 cm in order to avoid a type of background event which will be discussed later on.
4. Events which were not rejected up to this point, and which had a pion momentum in the Σ rest frame ≤ 166 MeV/c, were then analyzed by a physicist at the scanning table.

There are various reasons why the Σ decay track would have $P_{v.m.} \leq 166$ MeV/c:

(a) $\pi \rightarrow \mu$ Decay in Flight. For pions of lab momenta 180 MeV/c, we expect to see one pion decay in flight per 1000 Σ pionic decays per 1-cm pion travel path. Hence we expect a large number of these decays to appear in our data. In Fig. 1 we show the kinematics of $\pi \rightarrow \mu$ decays in flight for various pion momenta. The events which will add to the background are those that give rise to a muon momentum in the Σ rest frame ≤ 166 MeV/c. We note from Fig. 1 that those events have either a large decay angle in the lab frame ($> 5^\circ$)

⁴ R. F. Dashen, S. C. Frautschi, and D. H. Sharp, Phys. Rev. Letters 13, 777 (1964); P. Babu, *ibid.* 14, 166 (1965); E. Borchi, F. Buccella, and R. Gatto, *ibid.* 14, 507 (1965); S. P. Rosen and S. Pakvasa, *ibid.* 13, 773 (1964); D. Horn, M. Kugler, H. J. Lipkin, S. Meshkov, J. C. Carter, and J. J. Coyne, *ibid.* 14, 717 (1965).

⁵ U. Nauenberg, P. Schmidt, J. Steinberger, S. Marateck, R. J. Plano, H. Blumenfeld, and L. Seidlitz, Phys. Rev. Letters 12, 679 (1964).

⁶ These programs were developed at the Nevis Cyclotron Laboratories, Columbia University, by Dan Tycko and R. J. Plano.

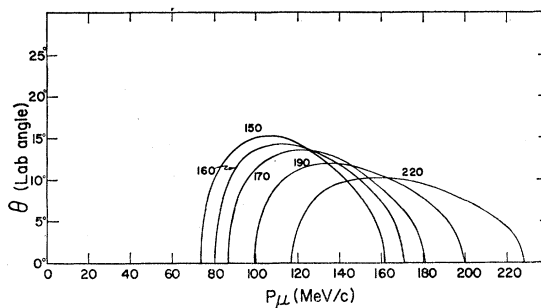


FIG. 1. Pion \rightarrow muon decay kinematics.

or give rise to a muon momentum much smaller than the initial pion momentum. This type of event is easily detectable if the pion has traveled more than 1 cm before it decays. We have detected a few $\pi \rightarrow \mu$ decays where the pion has traveled a distance < 1 cm, but we have not found any where the pion traveled $< \frac{1}{3}$ cm before it decayed. We therefore expect that the background is due to events where the pion decays before it has gone a distance of $\frac{1}{3}$ cm. In Fig. 2 we indicate how many of these background events we expect in a sample of 3×10^4 Σ^- decays.

(b) Pion Coulomb Scatterings. In the great majority of the events, the measured Σ decay track length is between 15 and 30 cm. Because of the magnetic field, these tracks turn through more than 17° in azimuth. Therefore at most half of these tracks that have a Coulomb scatter through the azimuthal angle $> 2^\circ$ can give rise to momenta < 166 MeV/c in the Σ rest frame. Nonetheless, these events with a "sudden" change in direction are easily detectable with curvature "templates" placed on the track. All events of this type can be clearly detected and do not add to the background.

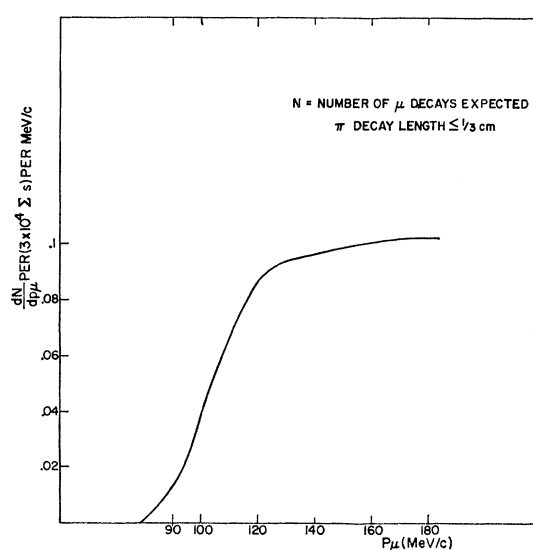


FIG. 2. Monte Carlo calculation of the muon momentum distribution in the decay $\Sigma^- \rightarrow \pi^- + n \rightarrow \mu^- + \nu + n$.

(c) *Multiple Scattering.* A pion from a $\Sigma \rightarrow \pi + n$ decay can suffer such a large number of small-angle scatterings that its measured momentum in the Σ rest frame becomes $< 166 \text{ MeV}/c$. These events cannot be distinguished from those where the pion comes from the Σ radiative decay. Hence we have to perform a background subtraction which is discussed later.

(d) Σ^- *Interactions.* The Σ^- can also interact with protons in the liquid and produce a Λ . These Λ 's are slow enough that they can decay near the production point so that the distance between the end of the Σ and the beginning of the Λ becomes undetectable (we choose the minimum visible distance to be 0.3 cm). In addition, the proton of the Λ decay could be so slow that it stops before leaving a visible track in the bubble chamber (we choose the maximum momentum of an invisible proton to be $80 \text{ MeV}/c$). These events look like Σ radiative decays with pion momenta $100 \text{ MeV}/c \leq P_{c.m.} \leq 120 \text{ MeV}/c$. The subtraction of these background events is discussed later.

(e) The event was incorrectly measured.

(f) The event is a true radiative decay, or (in the case of Σ^- decay) a lepton from the decay $\Sigma^- \rightarrow n + \mu^- (e^-) + \bar{\nu}$.

All these events, after being analyzed by a physicist, are remeasured and those that fit either hypothesis (a), (b), or (e) are rejected and are not analyzed any further.

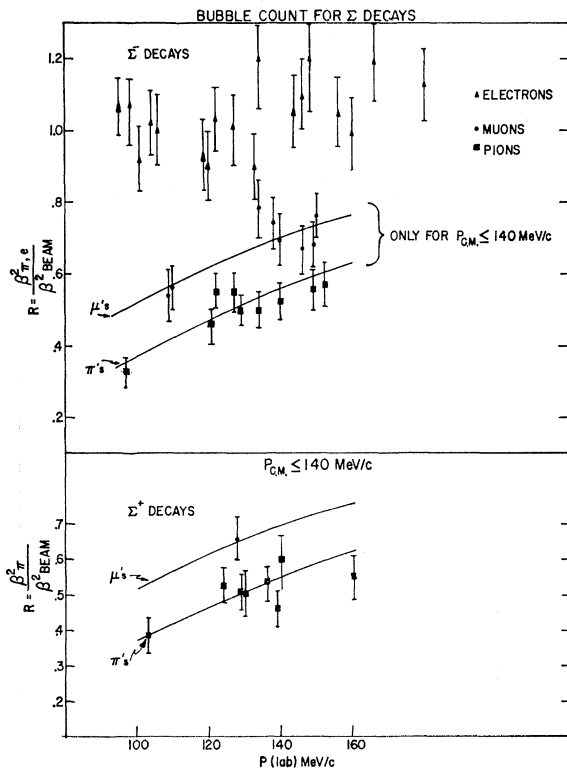


FIG. 3. Bubble count distribution of Σ decay tracks. The solid lines indicate the expected values of the ratio R assuming that the background beam tracks used for calibration are 450-MeV/c pions.

All other events with momenta still below $166 \text{ MeV}/c$ are then bubble counted.⁷ A distribution of the bubble count for decay tracks with $P_{c.m.} \leq 140 \text{ MeV}/c$ is shown in Fig. 3. The value of $140 \text{ MeV}/c$ was chosen arbitrarily as the limiting momentum for which one could distinguish pions from muons. Those decay tracks that stopped in the chamber were not bubble counted since their decay pattern can be used to classify them as pions, electrons, or muons. In the case of Σ^- decays, there were 27 events classified as electrons either from the bubble count or from their characteristic spiral track pattern in the bubble chamber. For Σ^+ decays there was only one such event found which has been described else-

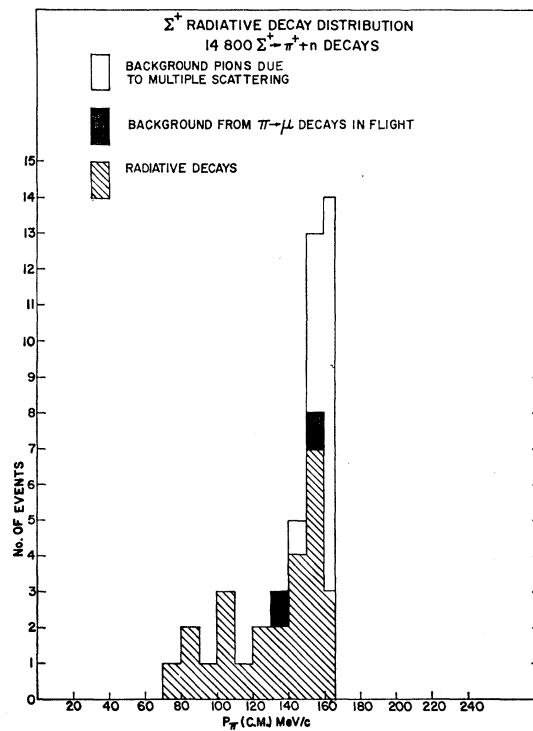


FIG. 4. The momentum distribution of Σ^+ decays with $P_{c.m.} \leq 166 \text{ MeV}/c$.

where.⁵ These 28 events are not included in the discussion that follows.

We have measured 14 800 $\Sigma^+ \rightarrow \pi^+ + n$ decays and 25 000 $\Sigma^- \rightarrow \pi^- + n$ decays for which all the cutoffs on track lengths and dips are satisfied. In this sample of data we have found 45 Σ^+ decays and 61 Σ^- decays where the decaying track had a momentum $\leq 166 \text{ MeV}/c$ in the Σ rest frame. Out of these events we have to subtract the background due to events of the type (a), (c), (d), and (f) (muonic Σ decays). The decay-track momentum distributions are shown in Figs. 4 and 5.

⁷ The bubble counting technique is described in Ref. 5.

Background Subtraction Due to $\pi \rightarrow \mu$ Decays in Flight and Due to Σ Muonic Decays

(1) Σ^+ Decays. The decay $\Sigma^+ \rightarrow n + \mu + \nu$ is forbidden by the $\Delta S = \Delta Q$ rule of the weak interactions and only one possible event in $\sim 10^5$ Σ^+ pionic decays has been observed.^{5,8} Hence the only background comes from $\pi \rightarrow \mu$ decays in flight. From a bubble count of Σ^+ decays with $P_{e.m.} \leq 140$ MeV/c, only one event is consistent with being a muon. This event is indicated in Fig. 3. From the curve in Fig. 2, we should have observed 1.6 events. This event has a lab momentum of 128 MeV/c and $P_{e.m.} = 132$ MeV/c. In addition, using the curve in Fig. 2, we expect 1 $\pi \rightarrow \mu$ decay between

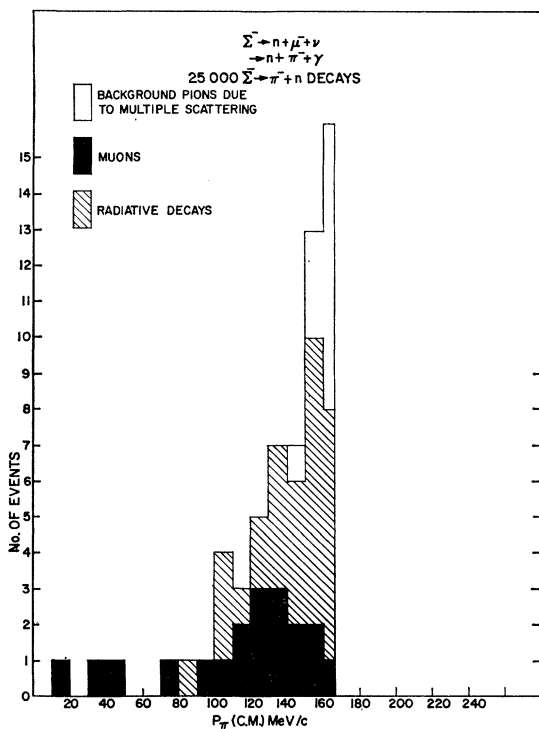


FIG. 5. The momentum distribution of Σ^- nonelectronic decays with $P_{e.m.} \leq 166$ MeV/c.

140 and 166 MeV/c. We subtracted (at random) an event with $P_{e.m.} = 154$ MeV/c.

(2) Σ^- Decays. For this case, the muon background is due both to $\pi \rightarrow \mu$ decays in flight and to the decay $\Sigma^- \rightarrow n + \mu^- + \nu$. The $\pi \rightarrow \mu$ decay background was determined using Fig. 2. We expect three events below 140 MeV/c and two events between 140 and 166 MeV/c. We have found 14 events where the decay track is considered a muon with $P_{e.m.} \leq 140$ MeV/c. Six of these stop in the chamber and decay into a characteristic electron and the other eight are considered muons from the bubble count. These eight are shown in Fig. 3. Since three of these 14 events are expected $\pi \rightarrow \mu$ decays in

⁸ W. Willis *et al.*, Phys. Rev. Letters 13, 291 (1964); A. Barbaro-Galtieri *et al.*, *ibid.* 9, 26 (1962).

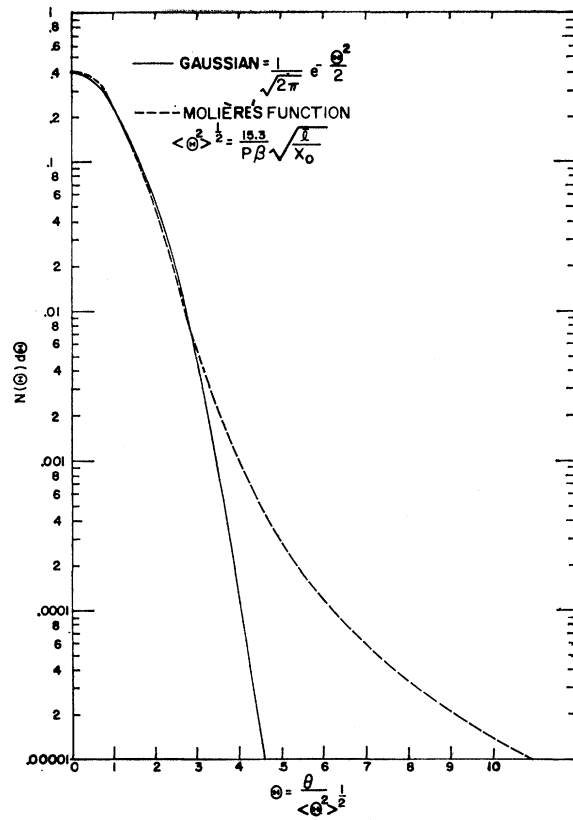


FIG. 6. Multiple scattering distribution according to the Gaussian and Molière theories.

flight, we have 11 $\Sigma^- \rightarrow n + \mu^- + \nu$ events which (assuming a constant-decay matrix element) gives a branching ratio to all Σ decays of $(0.56 \pm 0.20) \times 10^{-3}$. This is quite consistent with the known rate.⁸ We then determine, using only phase space, the number of these events expected between 140 and 166 MeV/c. We expect three events. The black boxes in Fig. 5 include all muons either from $\pi \rightarrow \mu$ decays in flight or from the Σ leptonic decay. The events with $P_{e.m.} \leq 140$ MeV/c are subtracted according to the bubble count while those with $P_{e.m.} > 140$ MeV/c are subtracted according to phase space and according to the curve in Fig. 2. The momenta of these subtracted events is presented in Table I.

Background Subtraction Due to Multiple Scattering

In Fig. 6 we show the relative probability of a track having been deflected through an angle θ as given incorrectly by the Gaussian distribution and as given correctly by the Molière theory in the manner described by Bethe.⁹ It is clear that for $\theta > 3 (\langle \Theta^2 \rangle^{1/2})$ the two curves disagree violently, the Molière theory predicting many more events with large θ than the simple Gaussian distribution. For the range of pion momenta and track

⁹ H. A. Bethe, Phys. Rev. 89, 1256 (1953).

TABLE I. List of events considered as muons in Σ^- decays.

Frame No.	P_{lab} (MeV/c)	$P_{\text{c.m.}}$ (MeV/c)
747494 ^a	29	18
651836 ^a	50	38
744085 ^a	47	46
659944 ^a	75	74
697975 ^a	98	98
654424	109	100
724662 ^a	103	120
723166	110	122
756258	134	112
334445	138	119
691000	146	129
305430	150	131
696727	140	137
711376	150	137
743724	147	149
545191	152	147
376122	154	153
712029	153	159
350318	164	160

^a Stop in the chamber and decay into an electron.

length in this experiment, the error in momentum due to measurement errors is 0.25 as large as the error due to multiple scattering, except for very short tracks ($l \approx 10$ cm) or very dipping tracks ($\lambda > 40^\circ$). Hence, since in addition all events with $P_{\text{c.m.}} \leq 166$ MeV/c are re-measured, the error in measurement can be neglected insofar as it contributes to the background for events with $P_{\text{c.m.}} \leq 166$ MeV/c. Also we neglected the effect of the measurement error on the shape of the pion momentum spectrum in the sigma rest frame. The width of the

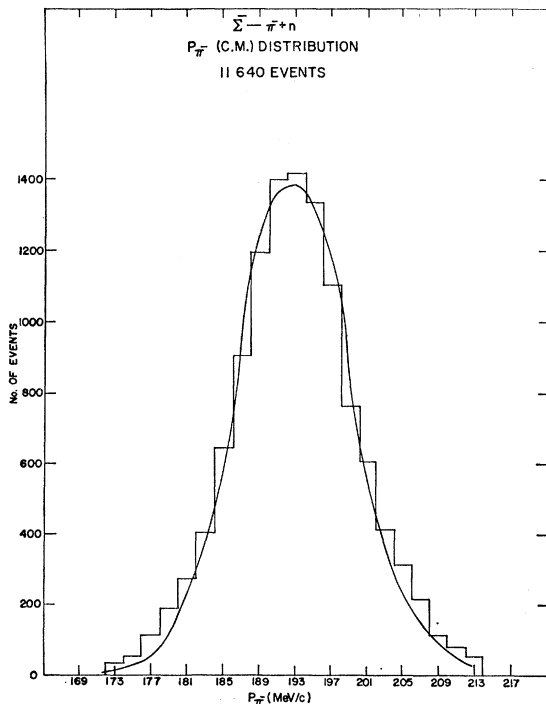


FIG. 7. Fit to the pion momentum distribution in the Σ^- decay rest frame using the Molière theory of multiple scattering.

theoretical spectrum as predicted by the Molière theory (there is an arbitrary constant that depends on the average length and average dip of the measured track) was adjusted until it gave a good fit to the major portion of the spectrum as shown in Fig. 7. Note that the fit for momenta below 180 and above 204 MeV/c is poor. This effect is due to the large measurement error of tracks which have short track lengths or large dips. This was checked by taking a sample of the Σ^- decay data with momenta below 180 and above 204 MeV/c and re-measuring them. It was found that half of the events in these momentum intervals had, on remeasurement, $P_{\text{c.m.}}$ between 180 and 204 MeV/c. Since we remeasure all events with $P_{\text{c.m.}} < 166$ MeV/c, we believe the fit to be adequate to obtain an accurate background subtraction. In Fig. 8 we show, using the fit obtained above, the expected distribution in $P_{\text{c.m.}}$ for Σ^- decays down to a momentum of 145 MeV/c. We use this curve to tell us how many events we have to subtract below 165 MeV/c as background due to multiple scattering. We do a similar fit to the Σ^+ decay data. The subtracted events are indicated as white boxes in Figs. 4 and 5.

Background Subtraction Due to Σ^- Interactions

There is a finite but small probability that a Σ^- might interact and give rise to background events of the type

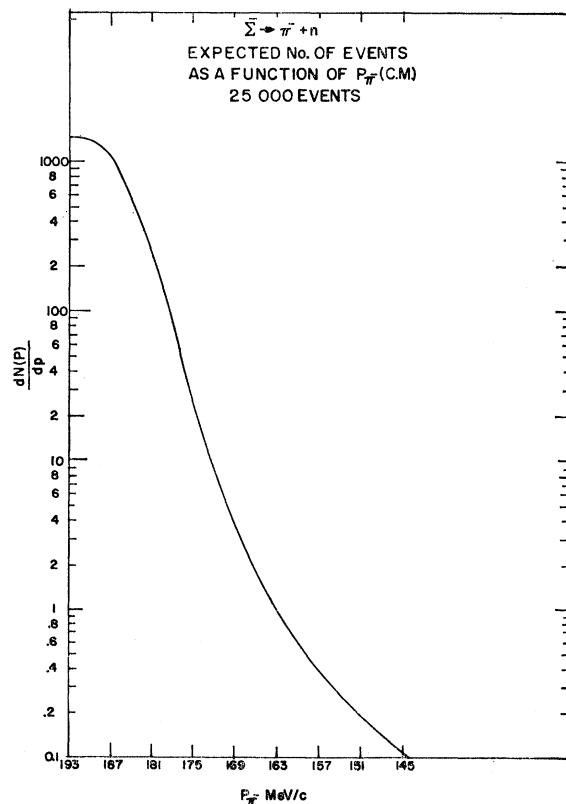
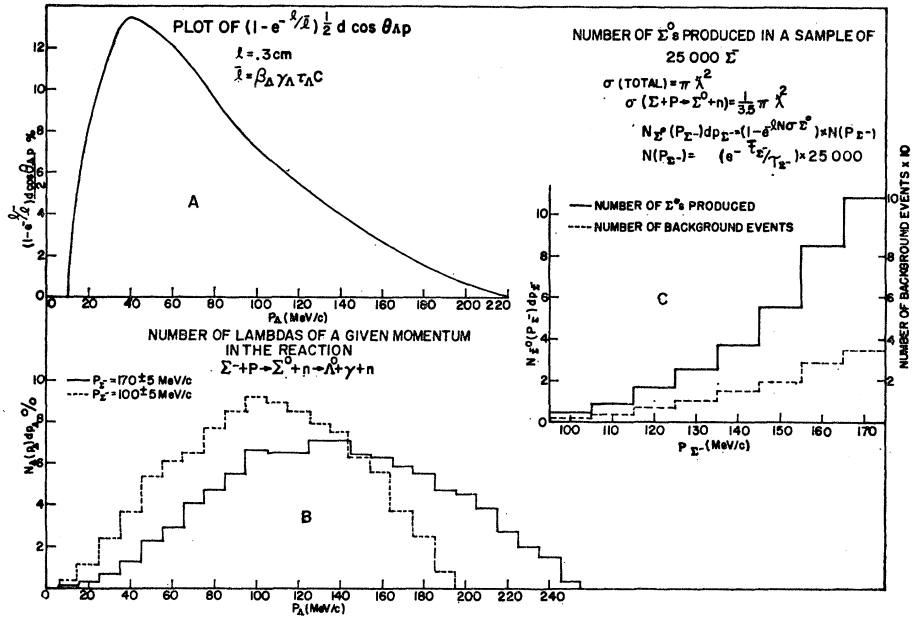


FIG. 8. Expected pion momentum distribution in the Σ^- rest frame down to a momentum of 145 MeV/c using the fit obtained in Fig. 7.

FIG. 9. Distributions used to determine the background from the reaction $\Sigma^- + p \rightarrow \Sigma^0 + n \rightarrow \Lambda^0 + \gamma + n$. (a) Probability that a given Λ^0 with momentum P_Λ will decay within 0.3 cm of its production point and, at the same time, that the proton from Λ decay will not be visible. (b) Λ^0 momentum distribution for two values of the Σ^- momentum by the Monte Carlo technique. (c) Calculation of the number of Σ^0 's produced in the reaction $\Sigma^- + p \rightarrow \Sigma^0 + n$ and calculation of the number of background events. The quantity t_{Σ^-} is the time it requires for the sigma to lose enough energy so that its momentum at the point of decay is P_{Σ^-} .



described in part (d). This background becomes very large if the Σ^- interacts at rest. Therefore we rejected all events where the Σ^- had a length > 0.95 cm. This ensures that Σ^- has not stopped before decaying or interacting. In Fig. 9, we indicate the relevant distributions required to calculate the number of background events. Figure 9(a) presents the probability, as a function of the Λ^0 momentum, that both the Λ^0 will decay before it has gone more than $\frac{1}{3}$ cm and that the proton in the decay is not visible (< 0.1 mm in length). The Λ 's produced in the reaction $\Sigma^- + p \rightarrow \Lambda^0 + n$ have $P_{\text{lab}} > 200$ MeV/c and hence do not contribute to the background. In Fig. 9(b) we show the expected momentum distribution, for two values of the Σ^- momentum, of lambdas produced by the reaction $\Sigma^- + p \rightarrow \Sigma^0 + n \rightarrow \Lambda^0 + \gamma + n$. These events can give rise to background. In Fig. 9(c) we show the number of background events expected after summing over the Λ momentum distribution and the Σ path length in a given momentum bite. We assume the absorption cross section is given by the unitarity limit $\pi \lambda^2$,¹⁰ and that the ratio of Λ^0 to Σ^0 production is 2.5.¹¹ The expected background after integrating over the Σ^- momentum is 1.2 events. The pion momenta in the Σ rest-frame range between 100 and 120 MeV/c. We subtracted the event with $P_{\text{o.m.}} = 110$ MeV/c as background.

After all the background subtraction we are left only with 26 Σ^+ radiative decays and 28 Σ^- radiative decays. The momenta of these events are presented in Tables II and III.

To determine whether the Σ^+ (Σ^-) pionic decays occur

via $P(S)$ waves or vice versa, we calculate likelihood distribution of C , the only parameter of the theory discussed in Ref. 1. In Fig. 10 we present the likelihood distribution of C for both the Σ^+ and Σ^- radiative decays. The theory described in Ref. 1 predicts that $C = M_\Sigma - M_n$ if the decay goes via the P -wave channel and $C = M_\Sigma + M_n$ if the decay goes via the S -wave channel. In the case of Σ^- decays we also performed the "likelihood" including the event with $P_{\text{o.m.}} = 110$ MeV/c

TABLE II. Σ radiative decays.

Frame	P_{lab} (MeV/c)	$P_{\text{o.m.}}$ (MeV/c)
745999 ^a	74	77
725644 ^a	79	86
249083 ^a	96	88
425127 ^a	89	93
380171	124	104
371839	130	107
403808	103	109
310583	136	117
176414	130	127
750696	140	129
22300	139	135
336376	160	135
424871	162	140
425926	174	144
695471	135	147
289895	143	146
683200	148	151
618947	130	152
743499	140	155
281404	170	156
203132	151	157
707256	173	158
679966	152	159
645455	146	162
694229	156	164
629633	177	165

^a Stop in the chamber.

¹⁰ We are assuming that at these low energies the absorption goes via the S -wave channel.

¹¹ We would like to thank Dr. R. Burnstein and Dr. G. Snow for this information.

TABLE III. Σ^- radiative decays.

Frame	P_{lab} (MeV/c)	$P_{\text{c.m.}}$ (MeV/c)
459988 ^a	78	88
746636 ^a	129	106
696288	97	109
350030	127	109
474498 ^b	120	110
394483	149	127
726339	134	128
708447	122	130
693861	128	135
685926	153	135
385974	140	138
350492	151	143
548856	143	144
709796	163	147
753015	166	148
732959	140	154
732302	150	154
386204	137	156
737947	137	156
697792	145	156
653670	141	157
751796	135	158
351753	150	158
393134	155	160
721713	170	160
689404	154	162
752884	147	166
293530	158	166
747789	161	166

^a Stop in the chamber.^b Event considered background due to the reaction $\Sigma^- + p \rightarrow \Sigma^0 + n$.

which was removed from the sample as background. The likelihood in this case does not differ appreciably from the one presented in the figure except that instead of $L(C=2100) = 2.5L(C=258)$, it becomes $L(C=2100) = 2.0L(C=258)$.¹² For Σ^+ decays the most likely value of C is 240 MeV, while for Σ^- decays the most likely value of C is ≥ 2000 MeV. In addition if the Σ^+ decayed by S wave we would expect only 20 events with $P_{\text{c.m.}} < 166$ MeV/c as compared to 24 events if it decayed by P -wave. For Σ^- decays we would expect 26 events if it decayed by S wave and 32 events if it decayed by P wave. To interpret these experimental results with some statistical significance, we make the following two assumptions: (1) the $\Delta I = \frac{1}{2}$ rule for non-leptonic decays is obeyed by Σ decays and (2) the pion momentum spectrum as calculated in Ref. 1 is essentially unaltered by form-factor effects.¹³ Now we can

¹² In addition, for the Σ^- radiative decays, we performed the calculation of the likelihood distribution of C including all the muons with $P_{\text{c.m.}} \geq 60$ MeV/c. The function used for the likelihood included (besides the radiative pion momentum distribution) the sigma muon decay momentum distribution as predicted by phase space with the rate as determined by Willis *et al.* (see Ref. 8), and the distribution of momenta of muons from $\pi \rightarrow \mu$ decays as indicated in Fig. 2. The likelihood distribution of C obtained this way was the same (up to a constant) as the distribution shown in Fig. 10.

¹³ We mention that magnetic-moment effects do not alter essentially the calculations in Ref. 1. See R. D. Young, T. Sakuma,

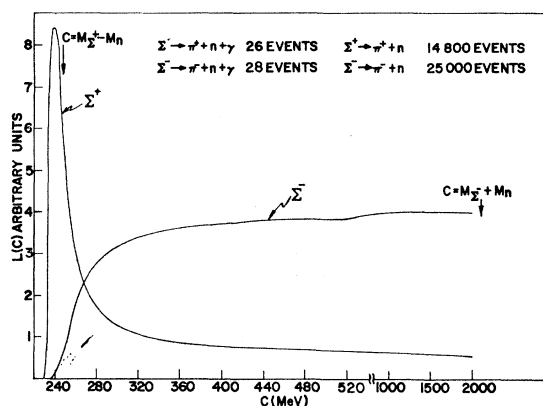


FIG. 10. Likelihood distribution of C for the Σ^+ and Σ^- radiative decay data.

state (using the product of the likelihoods) that the Σ^+ decay via the P -wave channel and the Σ^- decay via the S -wave channel is

$$\frac{L(\Sigma^+, C=250) \times L(\Sigma^-, C=2136)}{L(\Sigma^+, C=2128) \times L(\Sigma^-, C=258)} \times \frac{0.9}{0.5} \times \frac{5 \times 4 \times 0.9}{0.5 \times 1.6 \times 0.5}$$

equals 45 times more likely than the opposite combination of decay channels. The last two values of 0.9 and 0.5 represent the likelihood that the total number of Σ^+ radiative decays agree with the expected value. In the approximation that the product of our likelihoods is Gaussian this result is 2.7 standard deviations in favor of the decay-channel combinations indicated.¹⁴ This result is also in agreement with the prediction based on SU_3 or SU_6 .

ACKNOWLEDGMENTS

The Princeton group would like to thank Professor Jack Steinberger for the use of the film to carry out this experiment. In addition, we would like to thank Anthony Colleraine and Throop Smith for their help in various stages of the analysis. We would like to thank the staff of the 30-in. Bubble Chamber and Brookhaven National Laboratory for their help and cooperation during the exposure.

and M. Sugawara, Bull. Am. Phys. Soc. **10**, 467 (1965) and M. C. Li, *ibid.* **10**, 467 (1965) and University of Maryland Technical Report No. 451.

¹⁴ In the product of the likelihoods we have included the likelihoods of the integral rates as independent confirmations of the value of C . In the likelihood evaluation the integral rate is normalized to 1 so that the total rate dependence on C is lost. Therefore we believe it is reasonable to include the dependence of the integral rate on the parameter C as an additional confirmation of the most likely value of C independent of the likelihood derived from the momentum distribution.